Evolution of Electrohydrodynamic Flow of Suspended Particles in a Needle-to-Plate Negative DC Corona Discharge in Air

J. Mizeraczyk[1], A. Berendt[2], J. Podliński[2], and A. Niewulis[2,3]
[1]Department of Marine Electronics, Gdynia Maritime University, Poland
[2]Centre for Plasma and Laser Engineering, The Szewalski Institute of Fluid Flow Machinery, Polish Academy of Sciences, Poland
[3]Mathematics Teaching and Distance Learning Centre, Gdańsk University of Technology, Poland

Abstract—Corona discharges are used for collecting dust in electrostatic precipitators (ESPs). The dust collection is mainly realized by the electric forces which move the ionized dust particles to the collecting electrodes. However, the presence of corona discharge in the space between the charging and collecting electrodes in ESPs causes also the so-called ionic wind which set the gas molecules and dust particles in motion. As a consequence, a secondary electrohydrodynamic (EHD) flow is formed, which affects the primary flow of the dust-polluted gas and the collection of the dust particles.

In this communication we present images and velocity field maps and showing the temporal and spatial evolution of the EHD flow of the air and suspended dust particles in a needle-to-plate DC corona discharge arrangement, simulating an ESP. The measurements were mainly focused on the time period just after the corona discharge onset. The experimental apparatus for our study of EHD flow consisted of a needle-to-plate electrode ESP, high voltage power supply and standard 2D Particle Image Velocimetry (PIV) equipment.

The needle-to-plate electrode arrangement consisted of a needle (1 mm in diameter) electrode made of a stainless-steel, the end of which had a tapered profile with the tip having a radius of curvature of 75 μm. The interelectrode distance was 25 mm. Negative voltage of 8 kV was supplied to the needle electrode. An acrylic box, with the needle-to-plate electrode arrangement inside, was filled with air seeded with dust particles (incense smoke).

The flow and velocity field (PIV) images, recorded just after the corona discharge onset (in intervals from tens to hundreds ms) illustrate the temporal and spatial evolution of the EHD flow (air and the suspended particles) between the needle-to-plate electrode arrangement. They clearly show the formation of a ball-like structure of the particle flow at the needle tip and its evolution into a mushroom-like object moving with an average velocity of about 2.5 m/s towards the collecting electrode. This movement initiates a flow of the seeded air from the needle-tip vicinity into the space between electrodes. Then the EHD flow develops into two very regular vortices, rotating in opposite directions, and eventually the regular vortices disappear.

Keywords—DC corona discharge, EHD flow, flow measurement, PIV

I. Introduction

Corona discharges are used for collecting dust in electrostatic precipitators (ESPs). The dust collection is mainly realized by the electric forces which move the ionized dust particles to the collecting electrodes. However, the occurrence of a corona discharge in the space between the charging and collecting electrodes in ESPs causes also the so-called ionic wind which set the gas molecules and dust particles in motion. As a consequence, a secondary electrohydrodynamic (EHD) flow is formed, which affects the primary flow of the dust-polluted gas and the collection of the dust particles (e.g., [1]–[3]). The behaviour of secondary EHD flows have been extensively studied (e.g., [4]–[8]). Although the EHD motion of the dust particles in ESPs in the steady state (or time-averaged mode) has been well described theoretically and relatively well documented experimentally, there are scarce works on evolution and transient mode of the electrohydrodynamically-caused motion of the ESP gas. Still there is not clear how the ionic wind evolves after a high voltage is applied to the discharge electrode. An interesting experimental results on the ionic wind development in a needle-to-plate corona were presented in [9] where a high speed camera were used to capture images showing the evolution of ionic wind.

In this paper we present images and PIV flow patterns showing the temporal and spatial evolution of the EHD flows of the air and dust particles, suspended in it, in a needle-to-plate DC corona discharge. The measurements were mainly focused on the time period just after the corona discharge onset. Such study can be helpful in better understanding the EHD phenomena occurring in ESPs (dust particle deposition and reentrainment), and generally in EHD devices.

Corresponding author: Jerzy Mizeraczyk
e-mail address: jmiz@imp.gda.pl

Presented at the 2014 International Symposium on Electrohydrodynamics (ISEHD 2014), in June 2014

II. Experimental setup

The experimental apparatus for the study of EHD flow, shown in Fig. 1 consisted of a needle-to-plate electrode arrangement, simulating an ESP, high voltage supply and standard 2D Particle Image Velocimetry (PIV) equipment [10].

The needle-to-plate electrode arrangement consisted of a needle electrode made of a stainless-steel (1 mm in diameter), the end of which had a tapered profile with the tip having a radius of curvature of 75 μm. The grounded electrode was a stainless-steel plate. The interelectrode distance was 25 mm. A high-voltage DC power supplier model SL50PN300

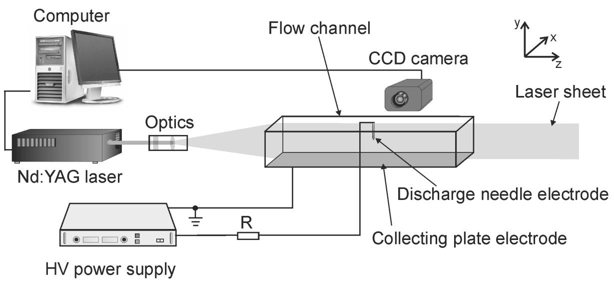

Fig. 1. The experimental setup for the measurement of EHD flow.

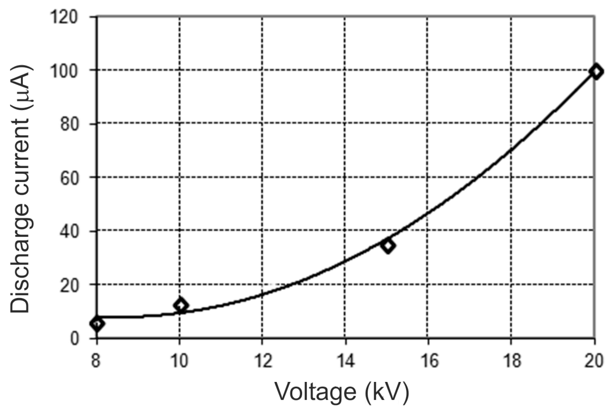

Fig. 2. Current voltage characteristics in the needle-to-plate arrangement measured with a dusty air for negative polarity.

(Spellman High Voltage Electronics Corporation) was used to run the discharge. Negative voltage of 8 kV (measured between the needle electrode and the collecting electrode) was supplied to the needle electrodes through a 3 MΩ resistor. The time-averaged glow corona discharge current was 6 μA. The discharge current-voltage characteristic for negative polarity is shown in Fig. 2.

An acrylic box, in which the needle-to-plate electrode arrangement was placed, was filled with air seeded with dust particles (incense smoke). In the experiments presented here, the case without forced axial flow was studied.

The PIV equipment consisted of a twin second harmonic Nd YAG laser system ($\lambda = 532$ nm), imaging optics (cylindrical telescope), CCD camera and computer for digital analysis of recorded images (Fig. 1).

PIV method enables determining the flow velocity vectors in a selected cross-section of the flow, called the observation plane. The observation plane is fixed in the flow by introducing into it a laser plane beam, called the laser sheet. If the laser sheet is assumed to be infinitely thin, a single CCD camera is used for monitoring the observation plane. This enables measuring two components of the velocity vectors which are parallel to the observation plane (the so-called 2D PIV case). The measurement of velocity vector field is based on the observation of the movement of flow seeding particles that cross the observation plane. The particle movement is determined by monitoring the laser sheet light scattered by the particles. The scattered laser light forms the flow image that is recorded by the CCD camera.

From two successive images of the observation flow the

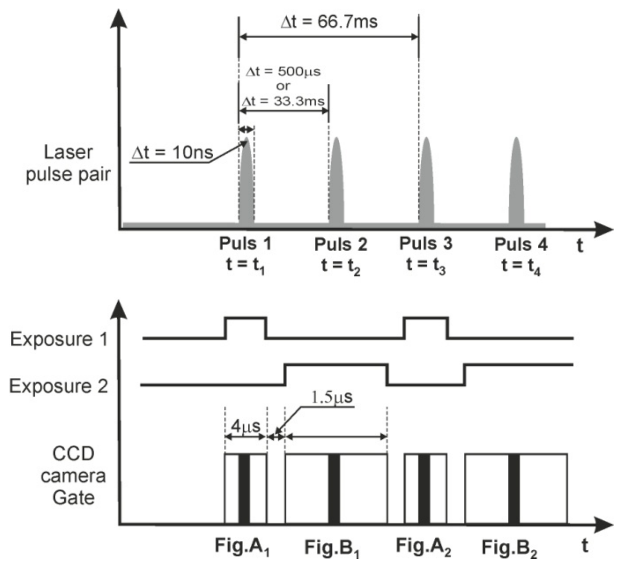

Fig. 3. Synchronization scheme of the laser and CCD camera.

velocity vector field of the seeding particles can be determined. When the seeding particles follow the gas flow, the seeding particle velocity field is assumed to be mapping the gas flow velocity field. In the other case, PIV method delivers the seeding particle velocity field in the flow. In our experiment the flow observation and PIV measurements were carried out in a laser-sheet plane (of a thickness of 1 mm) passing along the ESP box, close to the needle electrode and perpendicular to the collecting electrode.

The laser emitted a sequence of two very short-duration light pulses (a laser pulse pair). The repetition rate of laser pulse pairs could be controlled (Fig. 3). The duration of a single laser pulse was 10 ns. The minimum time between two pulses, consisting the laser pulse pair was 1 μs. In our experiment the time between two pulses in the pulse pair was set either 500 μs or 33.3 ms.

The former setting concerned the PIV measurements of flow patterns (i.e. flow velocity field and flow streamlines) while the latter corresponded to the recordings of instantaneous images of the flow. The repetition rate of the laser pulse pair was 15 Hz. It means that the minimum separation between onsets of two consecutive laser pulse pairs for the PIV measurements was 66.7 ms (this time was needed for data acquisition).

The CCD camera active element size was 1186×1600 pixels and it was synchronized with the laser beam pulse.

III. Results

Figs. 4 and 5 show typical instantaneous records of the flow and the flow patterns (i.e. flow velocity field and flow streamlines), respectively, in the transverse plane (the y-z plane, see Fig. 1) in the needle-to-plate electrode arrangement for different time elapses.

Images showing the temporal and spatial evolution of the EHD flow in the needle-to-plate electrode arrangement are shown in Fig. 4.

The images were taken from the discharge onset ($t = 0$) to a time of about 1.4 s. The effective exposure time of each

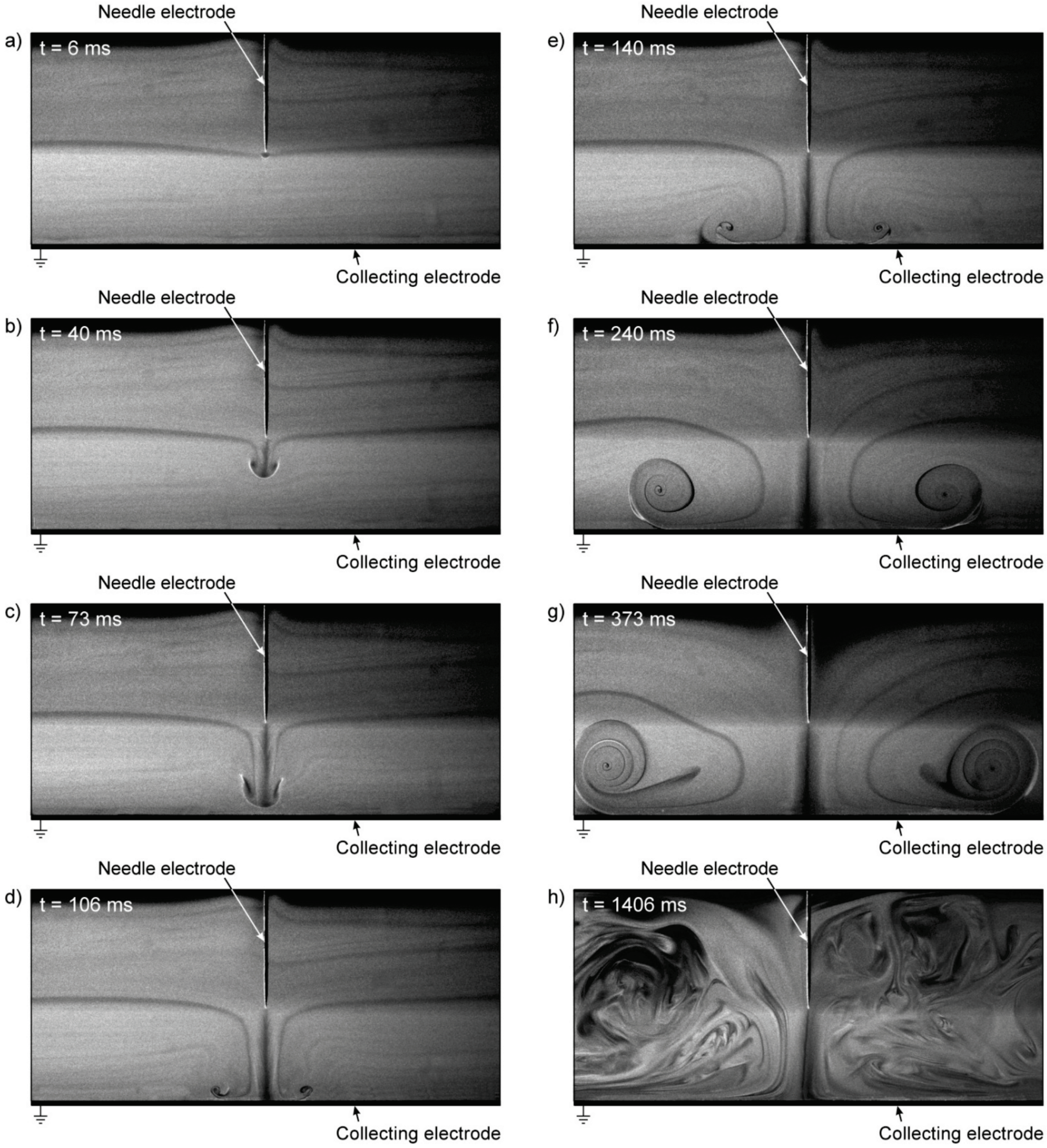

Fig. 4. Flow visualization. Evolution of the structures of the EHD flow after applying high voltage in the needle-to-plate arrangement in a still seeded air (instantaneous recordings of the laser green light scattered by dust particles). Negative voltage of 8 kV. Average total discharge current 6 μA.

image was about 10 ns (duration of the laser pulse). Each image is an instantaneous map of the laser green light scattered by the dust particles in the observation plane. High light intensity recorded in a given area of the image corresponds to a high dust concentration in this area. Dark spots or areas in the image means that there is no or little dust there. The image presented in Fig. 4a shows that the dust particle removal from the still seeded air (seen as a tiny dark ball, assuming the spherical symmetry) starts to develop in about $t = 6$ ms after applying the voltage. The other parts of the seeded air are not affected by the just applied electric field. After that the dust particles (seen as a very bright surface on the dark, i.e. dust-free mushroom-like moving object) are pushed from the needle electrode towards the collecting electrode (Fig. 4b).

It can also be noticed that the seeded gas from the needle-tip vicinity has started to flow into the space left by the dust particles. This may mean that a strong ionic wind has been created in the form of a cylinder from the needle-tip, forcing the seeded air from its vicinity to flow alongside. Thus a kind of jet moving towards the collecting electrode has been formed. After a time of about 80 ms the jet-like flow impinges on the collecting electrode (Fig. 4c).

With elapsing time the after-impinging processes develop and eventually two very regular vortices, rotating in opposite directions are formed (Figs. 4d-g). After a time of $t = 1.4$ s the vortices disappear (Fig. 4h). A kind of steady state settles.

Flow patterns (i.e. velocity field flow and streamlines) of the EHD flow in the needle-to-plate electrode arrangement are shown in Fig. 5. The particle flow patterns in the ESP box measured without applied voltage (results not presented

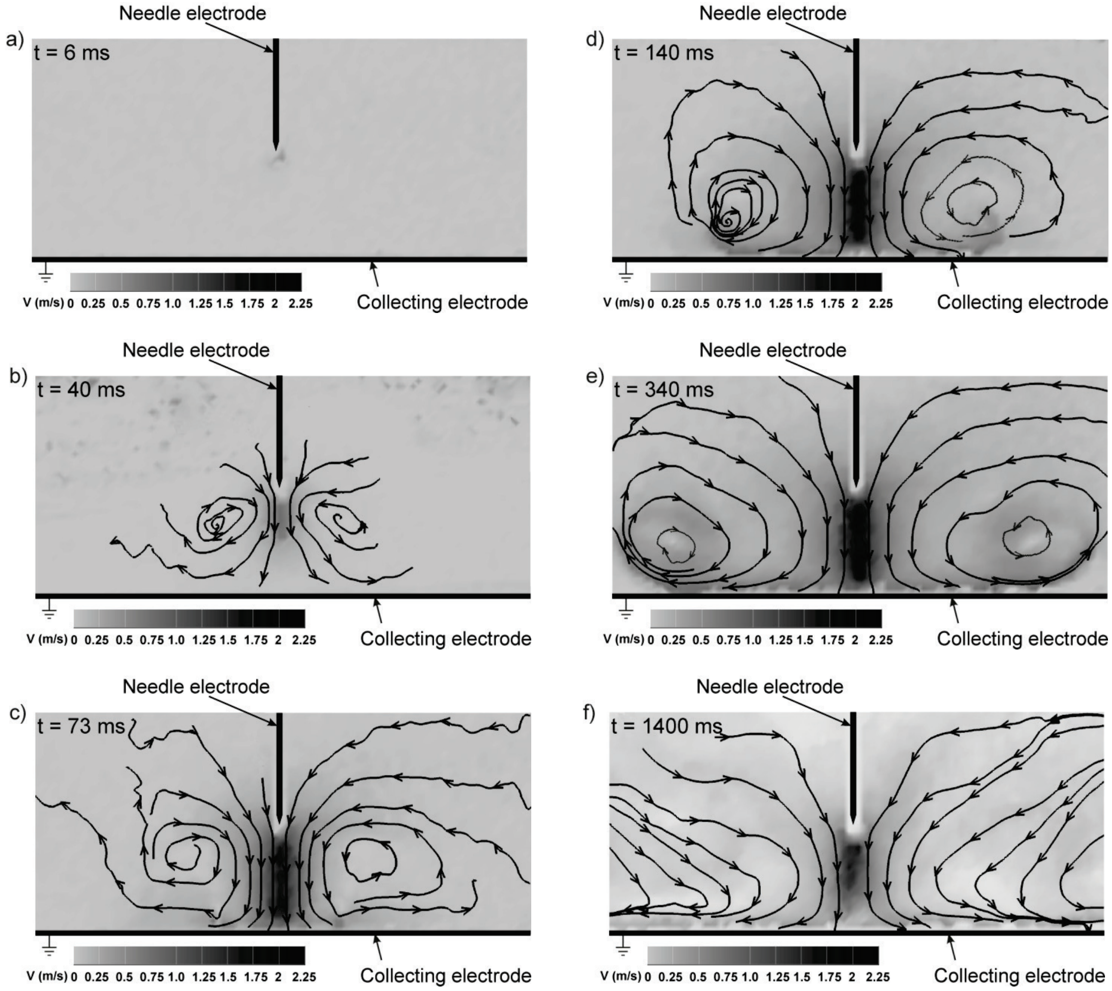

Fig. 5. PIV measurements. Evolution of the structures of the EHD flow after applying high voltage in the needle-to-plate arrangement in a still seeded air (instantaneous flow velocity field and velocity streamlines maps). Negative voltage of 8 kV. Average total discharge current 6 μA.

in this paper) showed that there was no movement of the dust particles in the y-z plane. This confirmed that the experiment has been started in the still seeded air (the dust particles were motionlessly suspended in the air). After applying a high negative voltage of 8 kV, particle EHD flow patterns started to develop around the needle electrode. After a time of 40 ms (Fig. 5b) the dust particles are pushed from the needle electrode downwards with a velocity up to 0.5 m/s. With elapsing time the velocity of the dust particles in the jet-like flow towards the collecting electrodes increases to about 2.5 m/s (Fig. 5e).

IV. Discussion

The evolution patterns of dust particle flow induced by the electric forces and ionic wind, presented in Figs. 4 and 5, resembles the development of a gaseous fuel wall-impinging jet injected by a high pressure into a combustion chamber [11]. It is interesting that a numerical simulation of the temporal evolution of charge density of EHD plumes induced by a blade electrode submerged in non-conducting liquid [12] gives similar structures.

Similarly as in the case of the wall-impinging jet, the evolution of the EHD flow presented in this paper, which we call an EHD jet for the purpose of this discussion, can be structurally divided into four stages: transient free jet stage (Figs. 4a-c), initial stage of wall-impinging jet (Fig. 4d), development stage of wall-impinging jet (Figs. 4e-g) and end stage of wall impinging-jet (Fig. 4h).

The time evolution of the transient free jet stage structures of the EHD flow in enlarged scale is shown in Fig. 6. Fig. 6 shows that the EHD jet is a laminar flow (Reynolds number is about 1000 based on the jet velocity and its dimension). It is interesting that the jet core is dark which suggests that the dust particle concentration is relatively low in it. In contrast, the bright surface of the mushroom-like moving object (Fig. 6, middle image) may suggest that the dust particle are pushed by the jet front.

After about 80 ms the initial stage of wall-impinging jet starts - the EHD jet tip arrives at the collecting plate electrode (Fig. 4d). Once the jet tip impinges on the plate electrode, the velocity and momentum of the jet tip decrease due to the still obstacle. Since the air accumulated at the impinging point has

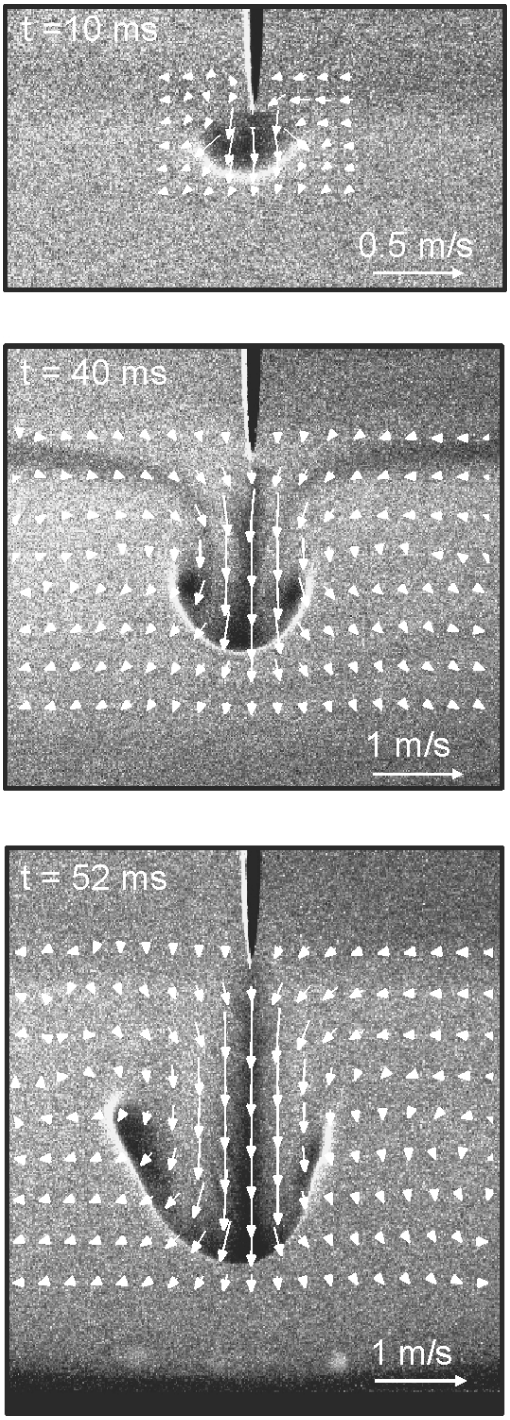

Fig. 6. Evolution of the transient free jet stage structures of the EHD flow.

low momentum, the following air of higher momentum pushes the low-momentum air along the plate electrode. However, the tips of the pushed air encounters the resistance from the surrounding air and roll up to become vortex cores.

In this way, two wall-region vortex cores are initially formed near the jet tip.

Figs. 4e-g shows the time evolution images of wall-impinging jet in development stage. In this stage the vortex cores are growing and forming into large-scale vortex struc-

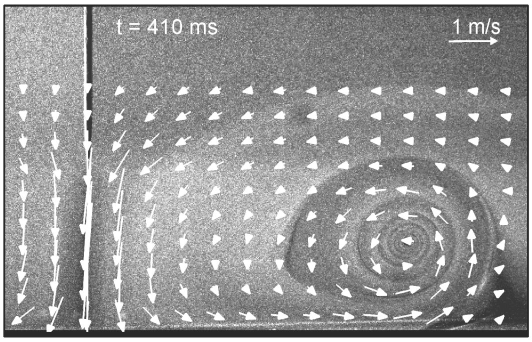

Fig. 7. Large-scale vortex structures in the development stage of wall-impinging jet.

tures with strong air-entrainment in the wall jet tip region. The vortexes are pushed away from the impinging point along the collecting electrode (Fig. 7).

The jet patterns in the end stage of wall-impinging jet are shown in Fig. 4h. It is seen that the wall vortexes have already dissipated their initial momentum in the surrounding air.

After this stage, if the corona discharge continues, a steady-state form of the EHD flow caused by the ionic wind settles in the whole ESP box. Fig. 5f (PIV measurements) the flow velocity field and flow streamlines of the structures of the EHD flow after establishing the steady-state. As mentioned above, in the steady-state there are no wall vortexes in the vicinity of the impinging point. Such a flow structure was also predicted by several numerical modellings of the steady-state EHD flow in air produced by electric corona discharges in the needle-to-plate ESPs (e.g., [13]).

V. Summary

The flow images and flow velocity fields, recorded just after the corona discharge onset (in intervals from tens to hundreds ms) illustrate the temporal and spatial evolution of the EHD flow in air with suspended particles between the needle-to-plate electrode arrangement. The images clearly show the formation of a particle flow ball-like structure at the needle tip and its evolution into a mushroom-like object moving with an average velocity up to 2.5 m/s towards the collecting electrode. This movement initiates a flow of the seeded gas from the needle-tip vicinity into the space between electrodes. Then the EHD flow develops into two very regular vortices, rotating in opposite directions. Eventually the vortices disappear and a steady-state form of the EHD induced by the ionic wind settles.

Acknowledgment

This work was supported by the National Science Centre (grant UMO-2013/09/B/ST8/02054).

References

[1] T. Yamamoto and H. Velkoff, "Electrohydrodynamics in an electrostatic precipitator," *Journal of Fluid Mechanics*, vol. 108, pp. 1–18, 1981.

[2] S. Masuda and S. Hosokawa, "Electrostatic precipitation," in *Handbook of Electrostatic Processes*, J.-S. Chang, A. J. Kelly, and J. M. Crowley, Eds. New York, NY: CRC Press, 1995, ch. 21, pp. 441–479.

[3] A. Mizuno, "Electrostatic precipitation," *IEEE Transactions on Dielectrics and Electrical Insulation*, vol. 7, pp. 615–624, 2000.
[4] P. Atten, F. Mccluskey, and A. Lahjomri, "The electrohydrodynamic origin of turbulence in electrostatic precipitators," *IEEE Transactions on Industry Applications*, vol. IA-23, pp. 705–711, 1987.
[5] T. Yamamoto, "Effects of turbulence and electrohydrodynamics on the performance of electrostatic precipitators," *Journal of Electrostatics*, vol. 22, pp. 11–22, 1989.
[6] J. Podliński, J. Dekowski, J. Mizeraczyk, D. Brocilo, and J.-S. Chang, "Electrohydrodynamic gas flow in a positive polarity wire-plate electrostatic precipitator and the related dust particle collection efficiency," *Journal of Electrostatics*, vol. 64, pp. 259–262, 2006.
[7] J. Mizeraczyk, J. Podliński, A. Niewulis, and M. Dors, "Laser investigations of flow patterns in electrostatic precipitators and nonthermal plasma reactors," in *Industrial Plasma Technology: Applications from Environmental to Energy Technologies*, Y. Kawai, H. Ikegami, N. Sato, A. Matsuda, K. Uchino, M. Kuzuya, and A. Mizuno, Eds. Wiley-VCH Verlag GmbH & Co. KGaA, 2010, ch. 5, pp. 49–64.
[8] J. Mizeraczyk, J. Podliński, A. Niewulis, and A. Berendt, "Recent progress in experimental studies of electro-hydrodynamic flow in electrostatic precipitators," *Journal of Physics: Conference Series*, vol. 418, p. 012068, 2013.
[9] K.-I. Tanoue, H. Taniguchi, and H. Masuda, "Experimental study on both ionic wind and resuspension of particles under unequal electrostatic field," *Advanced Powder Technology*, vol. 17, pp. 69–83, 2006.
[10] M. Raffel, C. E. Willert, S. Wereley, and J. Kompenhans, *Particle Image Velocimetry: A Practical Guide*, 2nd ed. Springer-Verlag Berlin Heidelberg, 2007.
[11] J. Yu, V. Vuorinen, H. Hillamo, T. Sarjovaara, O. Kaario, and M. Larmi, "An experimental investigation on the flow structure and mixture formation of low pressure ratio wall-impinging jets by a natural gas injector," *Journal of Natural Gas Science and Engineering*, vol. 9, pp. 1–10, 2012.
[12] P. Traoré, M. Daaboul, and C. Louste, "Numerical simulation and PIV experimental analysis of electrohydrodynamic plumes induced by a blade electrode," *Journal of Physics D: Applied Physics*, vol. 43, p. 225502, 2010.
[13] L. Zhao and K. Adamiak, "EHD flow in air produced by electric corona discharge in pin-plate configuration," *Journal of Electrostatics*, vol. 63, pp. 337–350, 2005.